U-Pb/Th-Pb Methodology

Monazite grains were extracted from whole rock samples using traditional methods of jaw crushing and pulverizing, followed by density separation using a Wilfley Table and heavy liquids (Methylene Iodide). The resulting heavy mineral fraction then undergoes separation using a Frantz LB-1 magnetic barrier separator to isolate the monazites. A representative split of the entire monazite yield of each sample is selected by hand under an optical microscope, and incorporated into a 1” epoxy mount along with multiple fragments of the primary and secondary monazite standards 44069 (WSM) and 554, respectively. The mounts are sanded down ~20 microns, polished progressively using a 9, 5, 3, & 1 micron polishing pads, and high resolution backscattered electron (BSE) images were acquired using a Hitachi S-3400N scanning electron microscope (SEM). Prior to isotopic analysis, the mounts are cleaned in an ultrasound bath of 1% HNO3 and 1% HCL in order to remove any residual common Pb from the surface of the mount.

U-Pb/Th-Pb geochronology of individual monazite crystals was conducted by laser ablation multicollector inductively coupled mass spectrometry (LA-MC-ICPMS) at the Arizona LaserChron Center (Gehrels et al., 2006, 2008). The isotopic analyses involved ablation of monazite using a Photon Machines Analyte G2 excimer laser (λ = 193 nm) coupled to a Nu Instruments HR-MC-ICPMS. Helium carries the ablated material into the plasma source of the ICPMS, which is equipped with a flight tube of sufficient width such that U, Th, and Pb isotopes are measured simultaneously. Analyses were conducted with a 5 micron laser spot diameter using an acquisition routine consisting of one 9 second integration on peaks with the laser off (for backgrounds), 9 one-second integrations with the laser firing, and a 30 second delay to ensure the previous sample is purged from the collector block. Operating parameters for the excimer laser were maintained at ~10 J/cm^2 at 5 Hz in constant energy mode for 65 laser bursts per analysis, producing an ablation depth of ~5.5 to 6 microns. Faraday detectors with 3x10^{11} ohm resistors measure ^{238}U, ^{232}Th, and discrete dynode ion counters measure $^{208-204}$Pb, all in static mode.

The errors in determining the ^{206}Pb/^{238}U and ^{206}Pb/^{204}Pb result in a final measurement error of ~1-2% (at 2-sigma level) in the ^{206}Pb/^{238}U age for each analysis. The errors in determining ^{206}Pb/^{207}Pb and ^{206}Pb/^{204}Pb also result in ~1-2% (at 2-sigma level) uncertainty in age for grains that are older than 900 Ma, however, they are substantially larger for younger grains due to the low intensity of the ^{207}Pb signal. The errors in determining the ^{208}Pb/^{232}Th and ^{208}Pb/^{204}Pb result in a final measurement of ~1-2% (at 2-sigma level) in the ^{208}Pb/^{232}Th age for each analysis.

The common Pb correction is accomplished by using the Hg-corrected ^{204}Pb and assuming an initial Pb composition from Stacey and Kramers (1975). Uncertainties of 1.5 for ^{206}Pb/^{204}Pb and 0.3 for ^{207}Pb/^{204}Pb are applied to these compositional values based on the variation in Pb isotopic composition in modern crystalline rocks. Interference of

^{204}Hg with ^{204}Pb is accounted for measurement of ^{202}Hg during laser ablation and subtraction of ^{204}Hg according to the natural $^{202}Hg/^{204}Hg$ of 4.35.

The 5 micron spot diameter in conjunction with the 9 second analysis routine (65 bursts at a 5Hz repetition) was used to minimize both spatial and at-depth mixing of multiple age domains. Grain selection and spot placements were based on the high resolution BSE images, for grains where there was a large difference in compositional domains multiple analyses were performed.

44069 (WSM) primary standard

The primary standard consists of individual monazite crystals with a well-calibrated $^{206}Pb/^{238}U$ ID-TIMS age of 424.9 ± 0.4 Ma and SHRIMP isotopic age of 426 ± 3 Ma (2-sigma) (Alienikoff et al., 2006). In-run analyses of these fragments are conducted twice following every set of five unknown measurements and the results are used to correct for inter-element fractionation of Pb/U and Pb/Th. U and Th concentrations are calibrated relative to the ID-TIMS measurements for 44069, which contains ~2005 ppm U and ~19800 ppm Th.

554 secondary standard

The secondary standard used for Th-Pb geochronology, consisted of individual monazite crystals with a $^{208}Pb/^{232}Th$ ID-TIMS age of 45.3 ± 1.4 Ma (2-sigma) (Harrison et al., 1999). In-run analyses of this secondary standard are conducted at the beginning and then periodically during the analytical run. The secondary standard yielded a mean 208Pb/232Th age of 46.8 ± 1.4 Ma (2-sigma) over the entire analytical session, shown in the plot below.

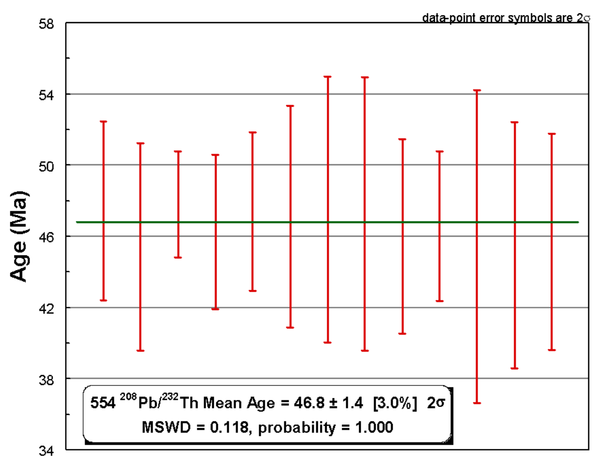

Precision and accuracy of monazite analyses

An offset plot that shows the precision and accuracy of U-Pb and Th-Pb analyses conducted by LA-ICPMS at the ALC, with respect to the published ID-TIMS or other analytical isotopic age, can be directly downloaded from https://docs.google.com/file/d/0B9ezu34P5h8ed1RCd0xSdjY2YjA/edit. Additionally, information and availability of the monazite standards used at the ALC is also available through the Geochronology Standards link on the main ALC website.

Results

The analytical data for each sample are reported in the following tables (accessible from the Project Page noted above). Uncertainties shown in these tables are at the 1-sigma level, and include only measurement errors.

Also included are plots that show the calculated ages of the primary standard analyzed with each sample. The ages are shown on Pb*/U concordia and Pb*/Th weighted mean diagrams using the routines in Isoplot 3.75 (Ludwig, 2012). The weighted mean diagrams show the weighted mean (weighting according to the square of the internal uncertainties), the uncertainty of the weighted mean, the external (systematic) uncertainty that corresponds to the ages used, the final uncertainty of the age (determined by quadratic addition of the weighted mean and external uncertainties), and the MSWD of the data set. These ages all show excellent agreement with the reported ID-TIMS 206/238 age of 424.9 ± 0.4 Ma.

Notes to accompany each data table are as follows:

1. Standard analyses with >10% uncertainty (1-sigma) in $^{206}Pb/^{238}U$ age are not included.
2. Standard analyses with >10% uncertainty (1-sigma) in $^{206}Pb/^{207}Pb$ age are not included, unless $^{206}Pb/^{238}U$ age is <600 Ma.
3. All uncertainties are reported at the 1-sigma level, and include only measurement errors.
4. Analyses conducted by LA-MC-ICPMS, as described by Gehrels et al. (2008).
5. U concentration and U/Th are calibrated relative to 44069 monazite standard and are accurate to ~20%.
6. Common Pb correction is from measured ^{204}Pb with common Pb composition interpreted from Stacey and Kramers (1975).

7. Common Pb composition assigned uncertainties of 1.5 for $^{206}Pb/^{204}Pb$, 0.3 for $^{207}Pb/^{204}Pb$, and 2.0 for $^{208}Pb/^{204}Pb$.
8. U/Pb and $^{206}Pb/^{207}Pb$ fractionation is calibrated relative to individual grains of 44069 monazite with an ID-TIMS age of 424.9 ± 0.4 Ma (2-sigma).
9. U and Th decay constants and U composition as follows: $^{235}U = 9.8485 \times 10\text{-}10$, $^{238}U = 1.55125 \times 10^{-10}$, $^{232}Th = 4.9475 \times 10^{-11}$, $^{238}U/^{235}U = 137.88$.
10. Weighted mean and concordia plots constructed using Isoplot 3.75 (Ludwig, 2012), with uncertainties reported at the 2-sigma level, and incorporate both the measurement and instrumental errors.

References:

Gehrels, G.E., Valencia, V., Ruiz, J., 2008, Enhanced precision, accuracy, efficiency, and spatial resolution of U-Pb ages by laser ablation-multicollector-inductively coupled plasma-mass spectrometry: Geochemistry, Geophysics, Geosystems, v. 9, Q03017, doi:10.1029/2007GC001805.

Aleinikoff, J.N., Schenck, W.S., Plank, M.O., Strogi, I., Fanning, C.M., Kamo, S.L., and Bosbyshell, H., (2006), Deciphering igneous and metamorphic events in high-grade rocks of the Wilmington Complex, Delaware: Morphology, Cathodoluminescence and backscattered electron zoning, and SHRIMP U-Pb geochronology of zircon and monazite, *Geol. Soc. Am. Bull., 118*, 39-64.

Harrison, T.M., Grove, M., McKeegan, K.D., Coath, C.D., Lovera, O.M., and Le Fort, P., (1999), Origin and episodic emplacement of the Manaslu Intrusive Complex, Central Himalaya, *J. Petrol., 40*, 3-19.

Ludwig, K., 2012, Isoplot 3.75: *Berkeley Geochrono9logy Center Special Publication 5*, 75.

Stacey, J.S., and Kramers, J.D., 1975, Approximation of terrestrial lead isotope evolution by a two-stage model: *Earth Planet. Sci. Lett., 26*, 207-221.